

# RSC Advances



This is an *Accepted Manuscript*, which has been through the Royal Society of Chemistry peer review process and has been accepted for publication.

*Accepted Manuscripts* are published online shortly after acceptance, before technical editing, formatting and proof reading. Using this free service, authors can make their results available to the community, in citable form, before we publish the edited article. This *Accepted Manuscript* will be replaced by the edited, formatted and paginated article as soon as this is available.

You can find more information about *Accepted Manuscripts* in the [Information for Authors](#).

Please note that technical editing may introduce minor changes to the text and/or graphics, which may alter content. The journal's standard [Terms & Conditions](#) and the [Ethical guidelines](#) still apply. In no event shall the Royal Society of Chemistry be held responsible for any errors or omissions in this *Accepted Manuscript* or any consequences arising from the use of any information it contains.

Mucoadhesive gel containing immunotherapeutic nanoparticulate  
satranidazole for treatment of periodontitis: development and its clinical  
implications

*AUTHOR NAMES: Yuvraj Singh <sup>1</sup>†, Parameswara R. Vuddanda <sup>1</sup>, Achint Jain <sup>1</sup>, Thakur P.  
Chaturvedi<sup>2</sup>, Sarita Parihar<sup>2</sup>, Sanjay Singh <sup>1</sup>\**

AUTHOR ADDRESS:

<sup>1</sup>Department of Pharmaceutics, Indian Institute of Technology (Banaras Hindu University)  
Varanasi – 221005, India.

<sup>2</sup>Department of Orthodontics, Faculty of Dental Sciences, Institute of Medical Sciences (Banaras  
Hindu University) Varanasi-221005, India.

†Present Address: Pharmaceutics Division, CSIR – Central Drug Research Institute, Lucknow,  
226031, UP, India.

\* CORRESPONDING AUTHOR

Office: +91-542-6702712

Fax: 91-542-2368428

EMAIL ADDRESS: [ssingh.phe@iitbhu.ac.in](mailto:ssingh.phe@iitbhu.ac.in)

**ABSTRACT:**

The aim of this study was to alleviate shortcomings in periodontal treatment by utilizing a mucoadhesive gel containing immunotherapeutic ganglioside coated polymeric nanoparticles (G-PNP) bearing satranidazole (SZ). Nanoprecipitation was used to fabricate SZ loaded G-PNP. In our previous deliberations aqueous dispersibility of conventional SZ had raised dose consistency issues. Usage of G-PNP allayed those fears as DSC and XRD data showed that SZ was rendered amorphous (more water dispersible than crystalline SZ) when captured in polymeric matrix of nanoparticles. G-PNP were added to sodium carboxy methyl cellulose (SCMC30 NP) gels and compared against SCMC 30 (gel containing conventional SZ) for texture, mucoadhesion, drug release and *inhibitory* susceptibility of *Aggregatibacter actinomycetemcomans*. Subsequently a 21 day single blind clinical trial comparing the efficacy of SCMC 30 NP and SCMC 30 was conducted. SCMC30NP showed maximum mucoadhesion force ( $43.27 \pm 4.10$ gf), low hardness ( $12.28 \pm .17$ N), moderate gel strength ( $8.53 \pm .21$ N) and elasticity ( $5.50 \pm 0.03$  mm). Well diffusion data revealed qualitatively greater antibacterial activity of SCMC30 NP. Dissolution studies demonstrated diffusion controlled release of SZ at concentrations above MIC. SCMC 30 NP caused significant ( $P < 0.05$ ) decrease in clinical markers of periodontitis, i.e. gingival index and pocket depth as compared to SCMC 30. Also reduction in plaque index produced by SCMC 30 NP was highly significant ( $P < 0.01$ ) as compared to SCMC 30 at end of 21<sup>st</sup> day. Amelioration of disease was improved due to Th-2 biased immuno shifting mediated by G-PNPs, which increased secretion of anti-inflammatory cytokines like IL-4 and TGF- $\beta$  from J774 macrophages. Clinical benefits incurred along with ease of application calls for scale up investigation of SCMC 30NP.

**KEYWORDS:** Periodontitis, satranidazole, PCL nanoparticles, ganglioside, immunotherapy, texture profile analysis

## 1. INTRODUCTION

Periodontitis is a set of inflammatory diseases afflicting the periodontium. It is instigated by bacterial load accumulated on sub gingival plaque. The subsequent inflammatory response inadvertently eats up surrounding tissue in an attempt to clear out bacterial debris produced by the initial immune response itself. Extensive supporting tissue damage results in extreme pain, deepening of periodontal pocket, tooth loosening and ultimately tooth loss<sup>1</sup>.

Primarily facultative anaerobic species<sup>2</sup> have been located in periodontal cavity and accordingly necessitate antibiotic intervention. Current treatment requires conjunction of exceedingly painful mechanical cleaning with systemic or localized antibiotic administration. Systemic antibiotics require high doses in order to be secreted substantially at a peripheral location like periodontal pocket. High antibiotic dose in turn causes unwanted side effects like hypersensitivity, gastrointestinal intolerance and development of bacterial resistance<sup>3</sup>. Therefore, a more satisfactory approach would be to administer antimicrobial drugs directly into the pocket by using a controlled release device. Local drug delivery limits the drug to its target site, with less or no systemic uptake. Unfortunately localized delivery to periodontal pocket is a tricky proposition as the flow rate of gingival crevicular fluid (GCF) perfusing from gums is greatly increased during periodontal infection. The site itself is very active (imagine the movement profile of regions pertaining to oral cavity) and is capable of dislodging a delivery device or washing away the released drug via salivary drainage. The most efficient dosage form then appears to be mucoadhesive gel perhaps, which would adhere to target site, and consequently would require lesser administration frequency.

Metronidazole (MZ) is the commonly used drug in management of periodontitis<sup>4</sup>, but is very bitter and leaves a metallic after taste<sup>5</sup>. Its marketed preparation requires several daily

applications ( promoting patient incompliance) paving the way for employing an alternative called satranidazole (SZ) which has milder taste and less nauseating influence<sup>6</sup>. SZ's potency is four fold higher than MZ when tested against gram negative anaerobes<sup>7</sup>. This very fact formed the basis of a study conducted previously by our group<sup>8</sup>. We found that mucoadhesive gel containing SZ was more effective in treatment of periodontitis than MZ gel; although low solubility of SZ interfered in its uniform dispersion in a hydrated gel, leaving room for dose inconsistency. Incorporation of SZ in polymeric nanoparticles (PNP) might render this hydrophobic antibiotic dispersible in aqueous media<sup>9</sup>. A study elsewhere has further observed that an initially high burst followed by a slower controlled and extended release profile of drug offered by polymeric nanoparticles can inhibit bacterial growth in 'biofilms'<sup>10</sup>. Incidentally, biofilms are a hallmark of periodontal infections<sup>11</sup>, and it is being hypothesized here that delivery of SZ in form PNP will tackle the inherent aqueous dispersibility issue of SZ along with providing a biphasic drug release effective in tackling periodontal bacteria.

Immune response is an extremely important event in etiologic progression of periodontitis. It has been reported that an elevated number of macrophages and antibody producing lymphocytes populate the gingival mucosa during chronic disease state. These interact in an aberrant manner to secrete pro-inflammatory T helper (Th1) cocktail of mediators (IL-12, TNF- $\alpha$ ) which not only aggravate the pre-existing disease burden but also interfere with production of anti-inflammatory T helper (Th-2) cytokines (IL-4, TGF- $\beta$ ) by feedback inhibition<sup>12</sup>. Gangliosides are endogenous neural phospholipids composed of ceramide and small sugar attached with one or more sialic acids residues; that have a unique capability of deflecting the immune regulation towards Th-2 response. If used as a formulation excipient, to produce ganglioside coated nanoparticles (G-PNP), there is a strong probability that surface exposed gangliosidic

components present in G -PNP will interact with gingival immunologic representatives to assert a Th2 dominant cytokine pattern, which in turn could accelerate disease remission<sup>13</sup>.

We consequently proceeded to develop a mucoadhesive gel system containing G-PNP of SZ which would be retained at application site, exceeding minimum inhibitory concentration of SZ required for anaerobes along with simultaneously exerting favourable immune response. Details of the pharmaceutical endeavours and the clinical outcomes obtained towards propounding the above hypothesis have been reproduced in the current manuscript.

## 2. MATERIALS AND METHODS

### 2.1. Materials

SZ was obtained as a kind gift sample from Alkem Laboratories Pvt. Ltd. Polycaprolactone, M.W. 40-45 kDa (PCL), Poloxamer 188 (PL188), Disialoganglioside from bovine milk(GD), Sodium carboxymethylcellulose (SCMC), carbopol 934P (CB934P), hydroxyl propyl methylcellulose (HPMC) K15, hydroxypropylcellulose (HPC), hydroxyethylcellulose (HEC) and dialysis membrane of molecular weight cut off 12 KDa were purchased from Sigma-Aldrich. Millipore Direct Q® 3UV water was used in all the studies.

### 2.2. Preparation of G-PNP

Nanoprecipitation method developed by Fessi, et al. <sup>14</sup> was modified for preparation of G-PNP. Entire operation was carried out at room temperature (25±1°C). The experimental design is portrayed in Table 1. Briefly, 30 mg of SZ and required amount of PCL to attain different drug to polymer ratios were dissolved in acetone (5mL) using a bath sonicator. Separately varying concentrations of PL188 (Table 1) and GD (0.1% w/v) were dispersed in 20 mL water. The organic phase was carefully loaded in a 23 gauge syringe and injected at rate of 10 mL/min into

the aqueous phase being stirred at 800 rpm. The milky nanosuspension (NS) thus formed was stirred for two hours at the same speed. NS was concentrated by removing acetone and excess quantity of water using a rotatory evaporator (IKA). Resulting suspension was monitored for particle size, zeta potential, and encapsulation efficiency to obtain the best optimized formulation. NS was stored in cold (2-8° C) refrigerated condition. Further, NS was gelsicated using lyophilizer (Lypholizer, Decibel, India) for 36 h at -40°C. The lyophilized G-PNP were stored in dessicator until used.

**Table 1:** Experimental array for G-PNP production

Batch	SZ(mg)	Drug Polymer ratio	Surfactant Conc. (%)	Stirring rate(rpm)	Injection Rate (ml/min)
S1	30	1:2	0.5	600	6
S2	30	1:2	1	800	8
S3	30	1:2	1.5	1000	10
S4	30	1:3	0.5	800	10
<b>S5</b>	30	<b>1:3</b>	1	1000	<b>6</b>
S6	30	1:3	1.5	600	8
S7	30	1:4	0.5	1000	8
S8	30	1:4	1	600	10
S9	30	1:4	1.5	800	6

### 2.2.1. Particle size, zeta potential, polydispersity index (P.D.I) and stability studies

The mean particle size, P.D.I. of the formulations was determined using Particle size analyzer, Delsa Nano C (Beckman Coulter, USA) functioning on dynamic light scattering technique. All samples were diluted in a 1:20 ratio with water to get ideal 50–200 kilo counts per second for measurements. Zeta potential was obtained by measuring the electrophoretic mobility of the particles under applied electric field. Measurements were made in triplicate at room temperature  $25 \pm 1^\circ\text{C}$ . The stability study of optimized batch was carried out at  $30^\circ \pm 2^\circ\text{C} / 65\% \pm 5\% \text{RH}$  for 90 days in a Thermo and Photo stability chamber. The change in particle size, P.D.I and entrapment efficiency was recorded after regular intervals.

### 2.3. Analytical method

Validated HPLC analytical method<sup>15</sup> was used for estimation of SZ. Estimation required RP-HPLC (Shimadzu, Japan) equipped with binary pumps (LC- 10 AT), and a UV-Vis dual absorbance detector (SPD-10A VP). The system was remotely operated using SCL-10 A class VP controller with chromatographic separation carried out on a Spherisorb ODS2 C18 column; 250×4.6 mm internal diameter, 5 $\mu$  particle size, functioning at room temperature. Mobile phase flowing at a rate of 1 mL/min in isocratic mode consisted of 10mM phosphate buffer/methanol (50:50 v/v) adjusted to pH 3 with 10% o-phosphoric acid solution. The detection wavelength was 294 nm. A run time of 10 min was fixed with SZ eluting at 4 min.

### 2.4. Transmission electron microscopy (TEM)

The optimized formulation of SZ loaded G-PNP was placed on a carbon coated copper grid and staining was done by a drop of 1% phosphotungstic acid<sup>16</sup>. Superfluous phosphotungstic acid on nanoparticles was wiped off by filter paper. The sample grid was dried at  $25 \pm 1^\circ\text{C}$ ; and viewed using a transmission electron microscope (TECHNAI 12 G<sup>2</sup> FEI Netherland), with images captured at appropriate magnification.

### 2.5. X- Ray diffraction (XRD)

XRD patterns of lyophilized G-PNP and pure SZ were obtained by employing X-ray Diffractometer (X'Pert PRO, PANalytical) using Ni-filtered Cu-K radiation, a voltage of 45 kV, a current of 30mA radiation. Patterns were obtained by using a step size of 0.001 per .05 s with a detector resolution in  $2\theta$  (diffraction angle) between  $5^\circ$  and  $60^\circ$  at  $25 \pm 1^\circ\text{C}$ .

#### 2.6.1. Total drug content (TDC)

Accurately measured 1 mL of NS was dissolved in 5ml acetone and diluted upto 50 mL with methanol. This solution was passed through 0.45 $\mu$ m syringe filter and assayed chromatographically to quantify the drug concentration ( $D_c$ ) using following equation.

$$TDC = (D_c \times Dilution\ factor \times Total\ volume\ of\ formulation)$$

### 2.6.2. Entrapment efficiency (E.E.)

Method employed by Jain, et al.<sup>17</sup> was used in determining E.E. The drug-loaded NS (500 $\mu$ l) was filled in upper chamber of Nanosep® centrifuge tubes fitted with an omega ultrafilter MWCO 30KD (Pall Life Sciences, India) and centrifuged (Cooling Centrifuge BL 24; Remi, India) at 5000 $\pm$ 10 rpm for 10 mins at -4°C. Filtrate was injected in HPLC to determine E.E.<sup>18</sup>.

$$Entrapment\ Efficiency\ (E.E.\ \%) = \frac{(A_t - A_{un})}{A_t} \times 100$$

$A_t$  = Total drug taken,  $A_{un}$  = Free SZ

### 2.7. In-vitro cytokine assay

Duo set elisa kits (R&D System, San Diego, CA, USA) were used for cytokine assay from J774 macrophages. Macrophages were maintained in RPMI-1640 medium (Sigma, USA) supplemented with 10% heat inactivated fetal bovine serum (FBS) 100 U/ml penicillin and 100  $\mu$ g/ml streptomycin at 37°C in atmosphere of 5% (v/v) CO<sub>2</sub>. Macrophages were seeded with a number of 1.5 x 10<sup>6</sup> cells/well in a 48 well plate. Plate was kept in incubator for 24 h at 37 °C to ensure adherence of cells to plate. Upon attachment media was aspirated and replaced with fresh media 1 h prior to treatment. G-PNP (0.25% SZ) and PNP (particles without GD coating but having same excipient and drug profile) were incubated with cells for 24 h. Following this the supernatant was collected and subjected to standard protocol of sandwich enzyme-linked

immunosorbent assays (ELISA) for estimation of secreted cytokines. Anti-cytokine antibodies and biotinylated mouse anti-mouse cytokine antibodies of TNF- $\alpha$ , IL-12, IL-4, and TGF- $\beta$  were used as primary and secondary antibodies respectively. Streptavidine-conjugated to horseradish-peroxidase was used as the developing reagent with tetramethylbenzidine as substrate. Cytokine concentration was estimated using calibration curves prepared using mouse recombinant TNF- $\alpha$ , IL-12, IL-4, and TGF- $\beta$ . Absorbance was measured using an ELISA plate reader at 450 nm. The experiment was performed in triplicate.

### 2.8.1. Preparation of Gel

Method of Varshosaz, et al.<sup>19</sup> was followed to prepare the gels. Weighed CB 934P was dispersed in 25 mL water. SZ dispersion in water was prepared separately and added to CB934P dispersion, concomitantly introducing gelling agent (SCMC, HPC, HEC, and HPMC) slowly under manual stirring. Gels were left overnight to afford solubilisation of the excipients, forming a visibly uniform structure. The concentration of SZ (0.25% w/v) was kept constant in all the batches. For preparation of gel containing G-PNP (correspondingly coded with suffix NP after their parent gel, for instance SCMC 30 NP) the method illustrated above was slightly modified by using NS of G-PNP instead of SZ dispersion. The experimental design is shown in Table 2.

**Table 2:** Experimental Design for manufacture of periodontal gels with their codes

Batch No.	CB934 P (gm)	SZ (gm)	HPMC (gm)	HEC (gm)	HPC (gm)	SCMC (gm)
HPMC 50	0.5	0.25	2.5			
HPMC 30	0.5	0.25	1.5			
HEC 30	0.5	0.25		1.5		
HEC 20	0.5	0.25		1		
HPC 5	0.5	0.25			5	
HPC 7.5	0.5	0.25			7.5	
SCMC 30	0.5	0.25				1.5
SCMC 20	0.5	0.25				1

### **2.8.2. Differential Scanning Calorimetry (DSC)**

DSC analyses were performed on optimized G-PNP (S5), SCMC30NP and SZ with differential scanning calorimeter (Perkin Elmer, USA). Sample weighing 5 mg was placed in hermetically sealed aluminium pans and heated at a rate of 22 °C/ min up to 250 °C under dynamic nitrogen purging.

### **2.8.3. TDC in gel**

Gel weighing 100mg was mixed in 100 mL water and filtered. 0.5 mL of filtrate was diluted to 5 mL with acetone and quantified chromatographically.

### **2.8.4. Mucoadhesion Force (MF)**

Arm balance was used for determining mucoadhesive capability of the gels. The apparatus consisted of a balance which held two plates made of glass on one side and a container with balancing load on the other side. The lower of the two glass plates was fixed to the base of the stage and upper plate was attached by a chain to the balancing arm. Goat intestinal membrane was obtained from local slaughter house, cleaned, perfused with saline and cut into appropriate size. Two pieces of membrane were attached to the lower glass plate and lower end of upper glass plate via adhesive, in such a way that mucosal side was exposed. Gel (100 mg) was placed on the membrane of the lower plate and the upper glass plate was placed over the lower plate and pressed with 35 g (preload) for 10 min. After removal of the preload, water kept in a burette at some height was allowed to drain into the balancing container till the glass plates detached. The weight of water required for detachment of plates was taken as mucoadhesion force.

### **2.8.5. Mechanical Properties by Texture Profile Analyser (TPA)**

The mechanical properties of gels were determined by TPA. The system was calibrated for probe, force and frame stiffness using Exponent®, a 32-bit software which drives the TPA.

Gels were transferred into a container and analysis was performed using a Stable Micro Systems Texture Analyser (TA-XT2®, Texture Analyser) mode in which the polymeric analytical probe (diameter 2 cm) was twice compressed (F1 and F2) into each sample at a defined rate ( $2\text{mm s}^{-1}$ ) to a depth of 15 mm with a triggering force of 4 g. The distance travelled by the probe at which the structure of gel undergoes irreversible deformity gives an idea about the elasticity of the system. A delay period (30 seconds) was allowed between the end of the first (F1 measures the hardness) and the beginning of the second compression cycle (F2 measures the gel strength). The work done in retracting the probe from gel gives an estimate of the adhesiveness. Entire cycle is figuratively depicted in supplementary material. From the resultant force-time plots, several mechanical properties including hardness, gel strength, elasticity and adhesiveness were derived<sup>20</sup>.

## 2.9. In-Vitro Release Study and Kinetics of Drug Release

SCMC30 and SCMC 30 NP with TDC within  $100\pm 10\%$  were used for in vitro release tests. Gel containing 2.5 mg SZ was taken in the centre of a dialysis bag which was then hermetically sealed and placed in a beaker containing 100 mL McIlvaine buffer pH 6.6 as dissolution medium. The entire system was kept at  $37\pm 1^\circ\text{C}$  under magnetic stirring at 100 rpm. Sampling was done at pre fixed time points for 24 hours. The dissolution profile so plotted was fitted to zero-order, first-order, Higuchi and Korsmeyer-Peppas equations to ascertain the kinetic modelling and mechanism of drug release<sup>21</sup>.

## 2.10. Anti-bacterial well diffusion assay

The antibacterial activities of SCMC 30 NP and SCMC30 were determined by slight modification of standard disk diffusion susceptibility test<sup>22</sup> on solid media by carving out small circular bores to easily accommodate gels. *A. actinomycetemcomitans* was used to evaluate the inhibitory potential and was acquired in freeze dried state from ATCC (ATCC Number 700685). It was reconstituted with 5 mL of Trypticase soy broth and then sub-cultured on Trypticase-soy-blood-agar (TSBA) plates (composed of 40 g/L Trypticase soy agar/ hemin 5 mg/L (bovine, Sigma Aldrich), N-acetylmuramic acid 10 mg/L and 10 % defibrinated sheep blood 50 ml/L), kept at 37° C under anaerobic conditions in the presence of 80 % N<sub>2</sub>, 10% CO<sub>2</sub>, 10 % H<sub>2</sub> for 72 h. The suspension turbidity was adjusted to  $1.5 \times 10^8$  cfu/ml. One hundred fifty microliters of this suspension was seeded onto TBSA media. Once the medium had solidified, a well, 4mm in diameter, was cut out of the agar and 100  $\mu$ l of SCMC 30 NP and SCMC 30, SZ solubilized in DMSO in various dilutions (Table 3) and blank inoculum made up of buffer only (serving as a negative control) were placed in the wells, in distinct plates, followed by incubation at 37°C under anaerobic conditions described above for 72 h. The dimension of the zone of growth inhibition around the treatment well was measured in mm. Any inhibition zone around the well measuring > 5 mm was considered a positive result.

**Table 3:** Numbers depicting mean diameter of inhibition zones in mm for gram negative antibacterial well diffusion assay.

Concentration( $\mu$ g/mL)	Mean diameter of inhibition zone (in mm), n=20			
	SZ	SCMC 30	SCMC 30 NP	Mcllvine Buffer
0.05	0	0	<5	0
0.1	<5	<5	10	0
0.25	12	13	25	0
0.5	38	40	64	0

## 2.11. Clinical Studies

A total of ten patients of both sexes, 21 years or above having been diagnosed as suffering from generalized or chronic periodontitis were selected for clinical evaluation (single blind, split mouth study design). Briefly, the mouth of selected patients was divided into two areas, groups A and B which was infected zones situated on opposite extremities of mouth creating a total of twenty experimental sites, ten in each group, and two per patient. Group A and B were treated with scaling and root planning, followed by application of SCMC30 and SCMC 30NP, respectively. Since in our previous deliberations we had established clinical superiority of mucoadhesive gel containing SZ over marketed MZ gel <sup>8</sup>, and considering the scope of trial(number of volunteers was limited), we refrained from using MZ gel as a control.

All the experimental sites were treated once daily. The gels were administered to the bottom of the periodontal pocket by using a disposable syringe equipped with rounded needle. The gels were injected into the pockets until the gel overflowed from the gingival margin.

Patients were cautioned not to brush in the area where the gel had been placed, not to chew rigid or sticky substances, and not to probe the area. The clinical parameters, such as probing depth (PD), plaque index (PI), gingival index (GI), were measured and scored before treatment initiation 0th day (baseline data) and on each 14th and 21st follow up day after treatment. An improvement in disease was indicated by any reduction in values of markers on 14th and 21st day to those which were recorded on baseline day. The studies were carried out in the Faculty of Dental Sciences, Institute of Medical Science, Banaras Hindu University, Varanasi, India. The necessary clearance was obtained to conduct above studies from the Institutional Human Ethical Committee of the same institute.

## 2.12. Statistical Analysis

For statistical comparisons one way analysis of variance (ANOVA) followed by Newman Keuls post-test and two way ANOVA followed by a multi comparative Bon-Ferroni post-test with  $p < 0.05$ ,  $p < 0.01$  and  $p < 0.001$  acting as different level of significance were applied using Graph Pad Prism® Version 5.01 software.

### **3. RESULTS AND DISCUSSION**

#### **3.1. Physicochemical Properties**

NS was milky white in appearance which meant that the greenish-yellow coloured drug had been properly captured in polymeric matrix, whereas the dispersion of SZ having the same drug content as that of NS showed traces of undissolved drug crystals in a yellow coloured solution. Preparing G-PNP of SZ thus solved the basic formulation barrier of potential dosing inconsistency due to precipitation and subsequent separation of SZ from mucoadhesive gel experienced during our previous efforts. The batches S1 to S9 were prepared according to design in Table 1.

##### **3.1.1. Effect of processing and formulation variables on G-PNP formation**

The injection rate, stirring speed, drug-polymer ratio and stabilizer concentration were found to affect the formulation features and their levels ascribed to in the orthogonal array were selected on the basis of preliminary experimentation. Each formulation and processing variable was varied so as to arrive at a unique combination, not replicated in any other batch. Figure 1(A) shows the data of particle size, PDI and Figure 1(B) shows E.E. and zeta potential obtained for different batches. The particle size was found in the range of 150 to 400 nm with zeta potential stretching from -12 mV to -20 mV. The negative charge can be attributed to the carboxylate group in the PCL backbone and the sialic acid residues in GD which coat G-PNP.

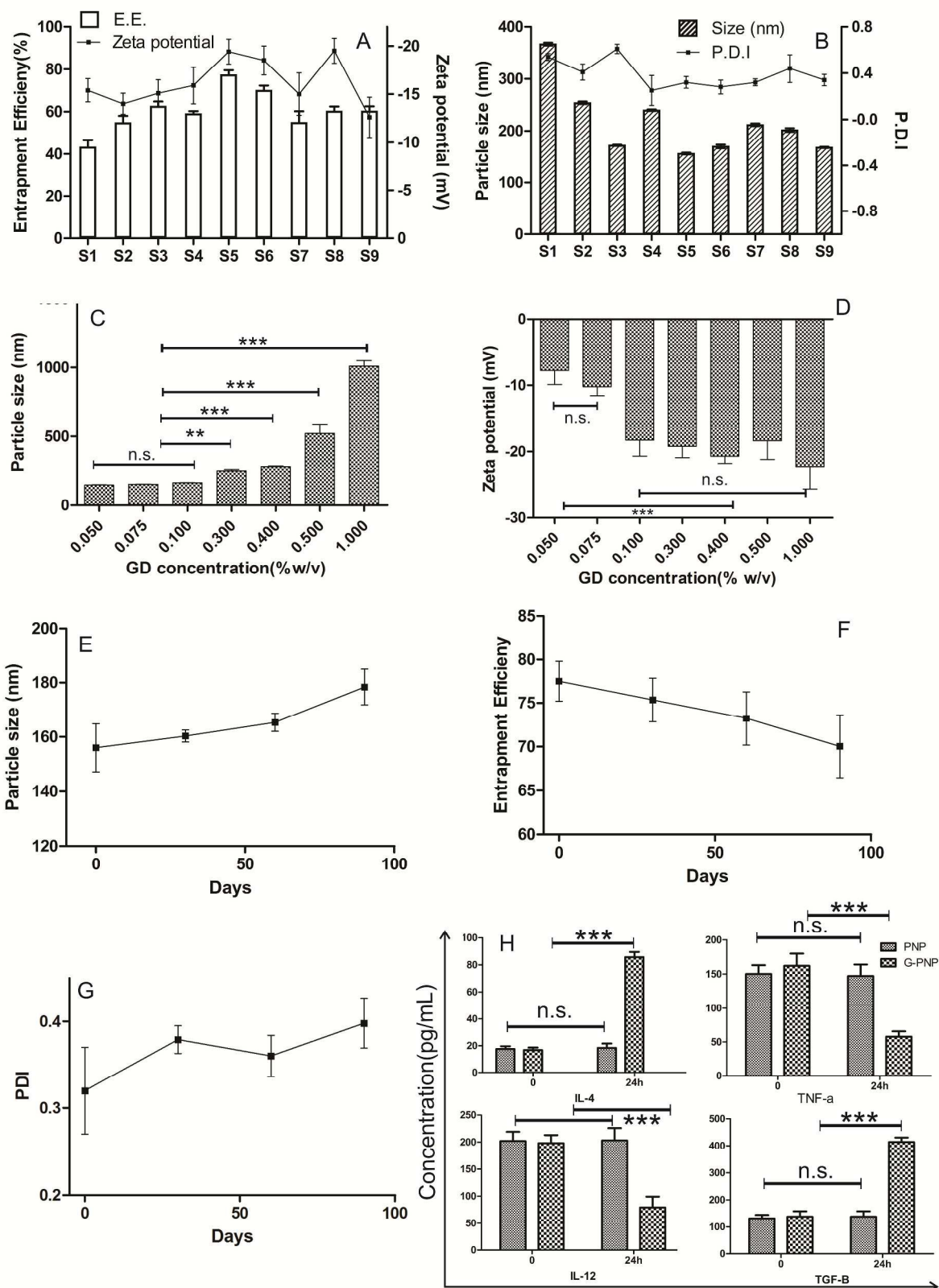


**Figure 1:** Graphics illustrating physicochemical characteristics and in- vitro cytokine inducing potential of developed G-PNP: (A) Entrapment efficiency and zeta potential of prepared batches. (B) Size and P.D.I of prepared batches. Considering the high E.E, low size of and relative invariability of P.D.I and zeta potential, S5 was selected as the optimized batch. (C& D) Effect of GD concentration on particle size and zeta potential of G-PNP. Significant increase in size between (0.1%) and (0.3%) onwards) suggested (0.1%) to be ideal concentration for coating. Similarly insignificant variation in zeta potential beyond (0.1%) suggested

the same. (E, F, G) Measurements of particle size, E.E and P.D.I during the course of stability study of S5. (H) In-vitro immunomodulatory responses in J774 macrophage secreted cytokine (TGF- $\beta$ , IL-4, IL-12, TNF- $\alpha$ ,) levels. The levels of cytokine released (pg/mL) in the culture supernatant were evaluated by sandwich ELISA after 24 h post treatment. (n=3; \*= $p < 0.05$ , \*\*= $p < 0.01$ , \*\*\*= $p < 0.001$ , n.s. = not significant, %values represent GD concentration in %w/v).

### 3.1.2. Surfactant concentration

At low surfactant concentration (0.5%; S1:  $367 \pm 2.67$ nm), an optimal surface coverage of the polymer droplets may not be achieved resulting in less stabilization of the particle dispersion and larger sizes. While at higher surfactant concentrations (1%; S5:  $156 \pm 1.87$ nm) the newly produced particles are fully covered by the surfactant molecules so there is less chance of particulate aggregation and particle size will not increase<sup>23</sup>. A too high concentration of surfactant molecule was not selected as the formulation was meant for internal use and could lead to mucosal damage<sup>24</sup>.

### 3.1.3. Optimization of GD concentration

Particle Size (Figure 1C) and zeta potential (Figure 1D) were also used to optimize appropriate GD concentration. Mean particle size of G-PNP increased from  $148.23 \pm 2.68$  to  $1009 \pm 52.68$  nm whereas zeta potential varied from (-)  $7.8 \pm 2.3$  to (-)  $22.3 \pm 5.1$ mV, when concentration of GD was increased (0.05 to 1.0%). Particles synthesized without GD had a mean zeta potential less than -5 mV, which suggested that GD was preferentially surface adsorbed leading to slight increment in negative zeta potential. Results suggested that 0.1% GD concentration was most appropriate for surface coverage. One way ANOVA followed by Newman-Keuls Multiple Comparison Test revealed that highly significant augmentation ( $p < 0.001$ ) in particle size was obtained if the GD concentration was increased beyond (0.1 % w/v). This might be due to the raised microviscosity of the aqueous media due to higher concentration of GD which interferes in movement of surfactant molecules. Zeta potential also varied significantly ( $p < 0.001$ ) when GD concentration

was increased upto 0.1% w/v, beyond which it ceased to vary suggesting complete coverage of G-PNP.

#### **3.1.4. Influence of Drug Polymer ratio on entrapment efficiency**

E.E. varied from 40 to 78% for different batches. Drug to polymer ratio had the starkest effect on E.E. S1 with a drug-polymer ratio 1:1 had an E.E of  $43.53 \pm 3\%$ . S5 with a drug polymer ratio 1:3 had an E.E of  $77.5 \pm 2.3\%$  and S7 with a drug polymer ratio 1:4 had an E.E of  $55.2 \pm 2.15\%$ . A low drug to polymer ratio (as in S1) does not capture SZ from all the sides, causing leakage of drug from polymeric matrix, whereas raising the polymer content too much (as in S7) promotes like-like hydrophobic interaction between polymer and rejection of drug molecule leading to generation of low drug entrapped particles. However, a balanced drug polymer ratio 1:3 in this study had the highest E.E. It may be attributed to appropriate quantity of polymeric carrier for drug entrapment.

#### **3.1.5. Injection Rate**

The injection rate was limited between 6 - 10 ml/ min. Using a very high injection rate caused phase separation as most of the organic phase was introduced at once into the aqueous phase providing inadequate time for diffusion of organic solvent preventing nanoprecipitation and causing separation of polymer.

#### **3.1.6. Stirring speed**

A range of 600 to 1000 r.p.m was selected. Stirring speed should be in adequate range; a too slow stirring speed, for instance 100 rpm does not produce strong enough convection currents in the aqueous media to continuously bring new surfactant molecules from the bulk in close vicinity of newly formed drug loaded polymeric droplets. Therefore, they cannot stabilize the suspension

by coating the newly formed interface. Higher stirring speed not only requires costly energy input but also causes agglomeration of polymer due to vortex formation. The vortex allows selective accumulation of organic phase leading to polymer- polymer interaction and phase separation. Therefore an intermediary range works just fine.

### 3.1.7. Selection of optimized batch S5

After monitoring the physico-chemical readings for all the batches ; S5 which had smallest particle size of  $156 \pm 1.87$  nm and highest E.E  $77.5 \pm 2.3\%$  with PDI of  $0.320 \pm 0.15$ , zeta potential of  $-19.4 \pm 1.1$  mV; was selected as the optimized batch. The selected batch was carried forward for further studies described in the current manuscript and was adapted universally for TEM, DSC, XRD, and inclusion in gel.

### 3.1.8. Stability of G-PNP

The stability study of optimized batch S5 was carried out at  $30^\circ \pm 2$  C /  $65\% \pm 5\%$  RH for 90 days. Polymeric nanoparticles showed stability with insignificant change in the particle size, E.E. and PDI (Figure 1E, 1F, 1G). Although small in magnitude, zeta potential ( $-19.4 \pm 1.1$ ) of the optimized batch was sufficient to stabilize the formulation because of PL188 which acts as steric stabilizer easily compensating for the small electrostatic repulsion.

## 3.2. In-Vitro Cytokine Assay

The macrophages after stimulation for 24 h with G-PNP and PNP were monitored for the level of TNF- $\alpha$ , IL-12, IL-4, and TGF- $\beta$ . G-PNP activated macrophages released 5-fold higher IL-4 and 3-fold higher TGF- $\beta$  after 24 h which instigate Th2 responses. The same cells expressed significantly lower levels of Th1 cytokines, IL-12(2.5 fold reduction) and TNF- $\alpha$  (2 fold

reduction) in 24 h. In comparison PNP treated macrophages did not induce any discernable variation in the basal cytokine levels (Figure 1H).

Immunological attributes of patient suffering from periodontitis is marked by elevation in level of pro-inflammatory Th-1cytokines (IL-12, and TNF-  $\alpha$ ) with simultaneous depression of anti-inflammatory Th-2 cytokines (IL-4, and TGF-  $\beta$ ) levels. We consequently gauged the level of several cytokines at *in-vitro* level to extrapolate the immunomodulatory activity of gangliosides to SZ loaded nanoparticles. Significantly elevated levels of IL-4, and TGF-  $\beta$  cytokines as well as decrease in level of IL-12 and TNF-  $\alpha$  expression were observed under *in-vitro* experimentation. As shown elsewhere gangliosides can be preferentially purported for this anti-inflammatory and Th-2 type response provocation<sup>13</sup>. The elevated levels of IL-4 in gingival mucosa can induce macrophage apoptosis, and its exogenous administration has even been proposed as a probable treatment protocol<sup>12</sup>. Overall this shifting of the Th1 toTh-2 response may be helpful for immunoadjuvant treatment of periodontitis.

### 3.3. XRD

The XRD pattern of SZ drawn in Figure 2(A) showed that the drug was crystalline in nature, with many characteristic peaks observed at  $2\theta$  of 10.64, 16.74, 17.97, 19.37, 21.20, 21.57, 22.90, and 24.32 and various minor peaks upto  $30^\circ$ . The peaks were very intense and sharp. The X-RD pattern of G-PNP, (Figure2B) shows that most of the characteristic peaks of SZ were absent, distorted, reduced in intensity or broadened. The dampening of diffraction intensity leads us to believe that the crystallinity is reduced<sup>24</sup> suggesting SZ's physical nature has been modified into amorphous form after entrapment in G-PNP.

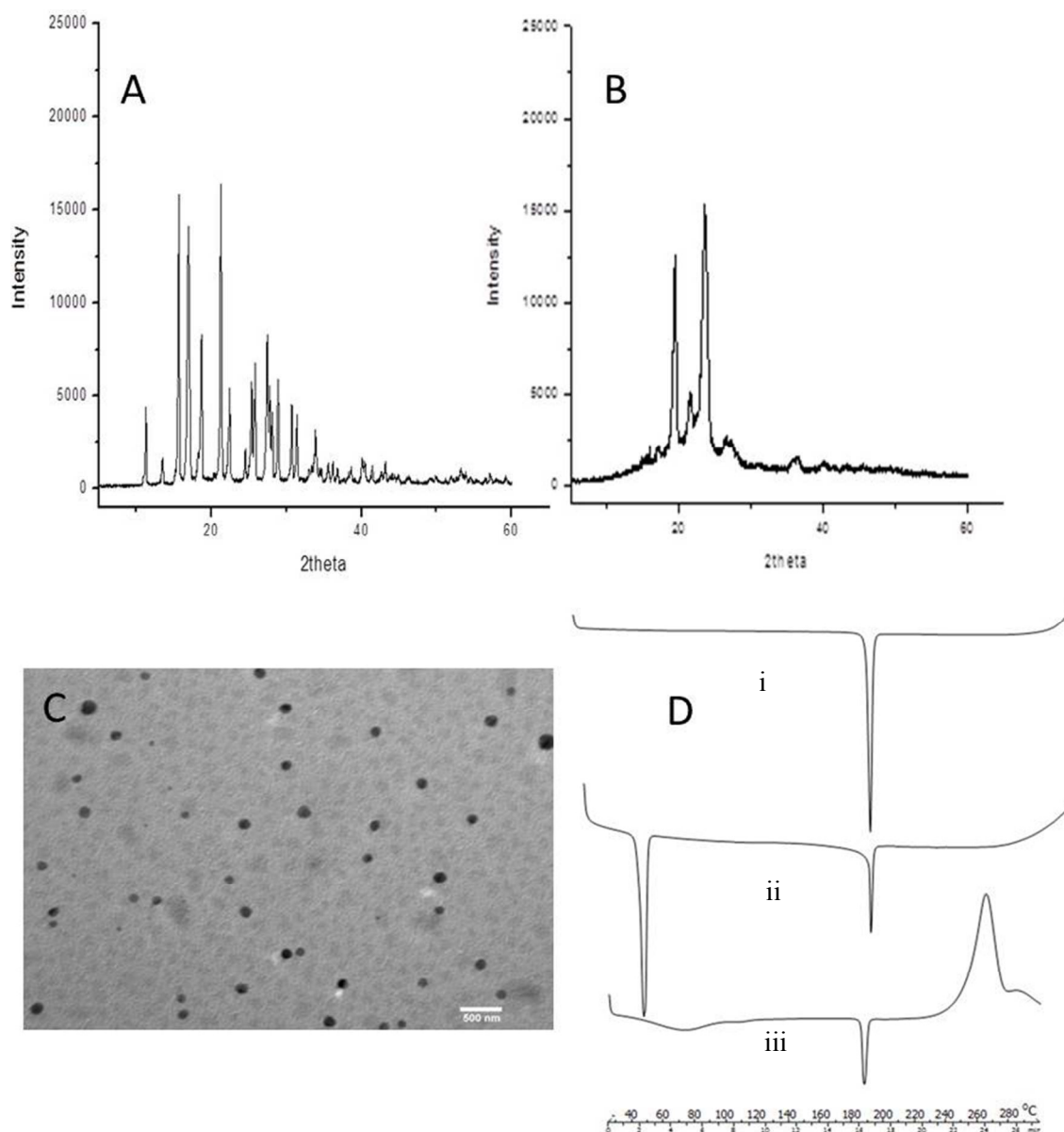


**Figure 2:** Characterization of G-PNP and SCMC NP. (A) Powder XRD spectra of SZ and (B) Lyophilized G-PNP. The crystallinity of SZ in (A) is clearly distorted in (B) suggesting amorphous nature of SZ. (C) TEM images of G-PNP (S5). The particles are mostly round and evenly distributed size wise. The particle size readings obtained by dynamic light scattering are in concordance with TEM measurements. The isotropic distribution of dark colour on particles is indicative of a matrix like drug polymer dispersion. Scale bar represents 500nm. (D) DSC thermograms of (i) SZ; (ii) lyophilized S5; (iii) lyophilized SCMC30NP made using S5. Characteristic peak of SZ at 186 °C is evident in all the curves, but its intensity is highly reduced in cases where SZ has been loaded in PNP or SCMC. (ii) Shows a sharp endothermic depression around mid-50's, which aptly shows that the bulk of the system is made up of PCL whereas it is absent in (iii), where SCMC is the major carrier.

### 3.4. TEM

The micrographs of G-PNP (S5), revealed (Figure 2C) that the particles are spherical in shape.

The particles have a uniform size distribution. The particle size was also in concordance with

those obtained by particle size analysis results. The equal distribution of dark colour on particles is indicative of a matrix like drug polymer dispersion.

### 3.5. DSC Studies

DSC curve of SZ shows a sharp endothermic peak at 186°C, its characteristic melting point [Figure 2D (i)]. Whereas an additional peak for PCL at 56 ° C (melting point) was obtained in DSC thermogram of lyophilized G-PNP. Further, the DSC thermogram of both G-PNP as well as its gel SCMC-30 NP exhibited the characteristic peak of SZ, albeit, with strikingly reduced intensity at 186°C [Figure 2D (ii) & (iii)]. The reduced intensity of peak of SZ indicates loss of sharp melting point due to conversion of crystalline SZ into amorphous form further backing the data obtained from XRD. It substantiates the claim that crystalline SZ has been rendered into amorphous form dispersed across small nanoparticles made of PCL. The implications of this subtle physical state modification were absolutely immense as it rendered SZ dispersible enough to form a uniform gel. The evidence to this phenomenon is presented in the comparative Figure 3(A & B). Note the greenish hue and the unevenly distributed SZ in SCMC 30 (panel A of Figure 3) which is replaced by the milky white appearance of G-PNP containing SCMC 30 NP.



**Figure 3:** Comparative photographs of (A) SCMC 30 and (B) SCMC 30 NP gels containing the same load of 0.25%w/v satranidazole. The improvement in aqueous dispersibility of SZ due to its incorporation in nanoparticles is clearly discernible with SCMC 30 NP. The uniform white colour of nanoparticle loaded gel is testament to entire gel containing evenly distributed

SZ bearing G-PNP. However selective localization of drug in SCMC 30, due to its non-solubility in water raised the probability of dose inconsistency.

### 3.6. Mucoadhesion Force

The results of MF measurement for different gels are shown in Figure 4A. SCMC30 ( $44.46 \pm 5.20$  gf), SCMC 30 NP ( $43.27 \pm 4.10$  gf) and HEC30 ( $41.10 \pm 7.40$ gf) showed the highest values amongst all the gels. HPMC 50 ( $38.98 \pm 7.90$  gf) and HPMC 50 NP ( $32.56 \pm 4.60$  gf) also exhibited substantial mucoadhesivity but were not considered on grounds of other parameters. Gels made of HPC ( $12.43 \pm 2.5$ gf) had very low mucoadhesive capability. Carbopol resins readily swell in water exposing a large adhesive surface for maximum contact with mucin (the glycoprotein predominant in the mucous layer) and, thus, provide efficient mucoadhesiveness. It was further found that, MF increased with concentration of polymers SCMC and HEC which themselves are mucoadhesive; SCMC 20 had a reading of  $24.00 \pm 4.60$  gf whereas SCMC 30 required  $44.66 \pm 5.20$  gf to detach the two plates. Using G-PNP did not produce any noticeable change in MF. Since G-PNP are formed of PCL which is relatively non-bioadhesive<sup>25</sup> and consequently do not influence mucoadhesive strength of the system. Gel showing highest MF was expected to be retained for the longest duration of time at site of infection.

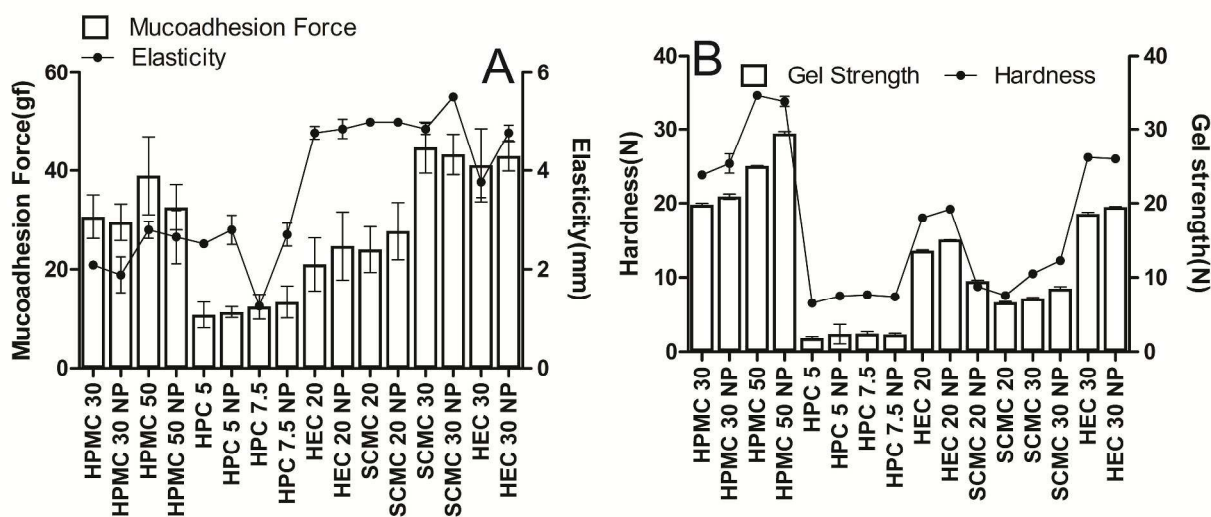


**Figure 4:** Parameters obtained from TPA and mucoadhesion testing; these were used in selection of optimized gel. HPMC gels were very hard, whereas HPC gels were almost fluid. SCMC constructed gels exhibited highest mucoadhesion force, elasticity and moderate to low gel strength, prompting their selection for clinical testing. HEC had comparable properties to those of SCMC gels but its high hardness meant that it would pose problems during dispensing and was consequently not used further.

### 3.7. Mechanical Characterization of Gels by TPA

TPA was used to characterize the mechanical properties of prepared gels. This simple and rapid technique provided information related to elasticity, hardness and gel strength, (Figure 4A and 4B respectively). The gels of HPMC 50 ( $34.63 \pm 0.11$ N), HPMC 50 NP ( $33.80 \pm 0.67$  N) series were the hardest followed by HEC30 ( $26.19 \pm 0.02$  N), HEC 30 NP ( $25.99 \pm 0.08$ N) made gels. SCMC 30 ( $10.51 \pm 0.25$ N), SCMC 30 NP ( $12.28 \pm 0.17$ N) were a moderate third. HPC gels barely registered on the hardness and elasticity scale: penetration only up to  $2.52 \pm 0.08$  mm (HPC 5),  $2.80 \pm 0.30$  mm (HPC 5NP), until the structure of gel broke. This was not unexpected as HPC gels were almost fluid, which meant that had high propensity to loose shape. Counter intuitively gels made of HPMC also had very low elasticity ( $1.89 \pm 0.36$  mm to  $2.65 \pm 0.54$  mm); this was due to rigid nature of gel which necessitated stress induced structural deformity for the probe to move. The elasticity of gel series made of HEC and SCMC was similar, in fact HEC and SCMC matched in terms of all the mechanical properties except hardness. Non elasticity of gels manifests itself as cracked or brittle structure seen in transparent bottles of marketed hair gels. It is not a big issue in cosmetology, but for cases relating to medicated gels there is a strong chance of drug expulsion or at least uneven drug release pattern.

Ideally formulations designed for periodontal delivery should have low hardness, yet high adhesiveness, and elasticity. Low gel hardness (advantage of SCMC 30 over HEC30 ) will reduce the effort required to remove the gel from the container and application onto the oral mucosa, whilst high gel mucoadhesiveness will produce prolonged retention of the gel onto the oral mucosa<sup>20</sup>. SCMC 30 and SCMC 30 NP had the highest value of MF, adhesiveness, and

moderate elasticity with comparatively less hardness prompting us to select it as the final formulation for clinical study.

### 3.8. In-Vitro Drug Release Studies and Kinetic Modelling

SCMC 30 showed initial burst release of SZ with 30% of release in first hour followed by a slower more sustained release extending up to 24 hours when at least 99% of TDC was released. SCMC 30 NP produced a higher initial burst release 40- 45 % in first hour itself followed by a slower extended release where about 75-80 % drug is released up to 24 hours (Figure 5).

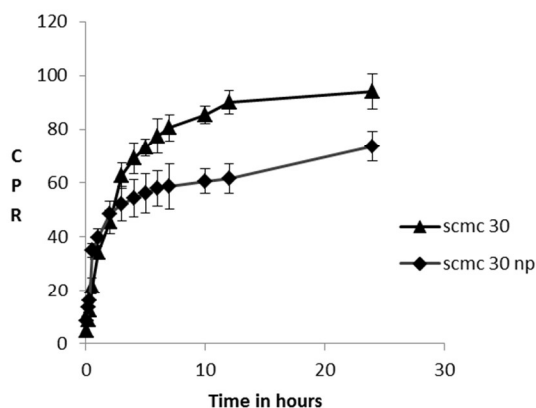


**Figure 5:** Comparative dissolution profile for SCMC 30 and SCMC 30NP. The initial burst release of SZ is more evident in SCMC 30NP due to presence of surface adhered nanomeric drug. However once the free drug is exhausted controlled release kicks in exercising significant restriction, reflected in only 70 % drug released by SCMC 30NP over 24 h, whereas SCMC 30 is almost completely exhausted. Here CPR is cumulative percentage of SZ released against time.

The kinetic data with  $r^2$  values obtained for different models is depicted in Table 4. The best fit was obtained in Korsmeyer- Peppas model (highest  $r^2$  values). The n values for Korsmeyer- Peppas equation for SCMC 30 was more than .5 which showed drug release mechanism to be a combined effect of erosion and drug diffusion. This is expected as SCMC is hydrophilic, water swellable and gets rapidly eroded. More concentrated gels were reported to dissolve at a slower rate in the dissolution media than less concentrated ones because of hindrance in media entry created by tortuous polymeric strands more prevalent in concentrated systems.

**Table 4:** Kinetic modelling for different batches of gels

Batch ID	r <sup>2</sup> Value			Korsmeyer Peppas	
	Zero order	First order	Higuchi	r <sup>2</sup> Value	(n)* value
SCMC 30	0.59	0.86	0.86	.98	0.65
SCMC20	0.36	0.85	0.81	.96	0.6
SCMC 30 NP	0.55	0.76	0.91	.96	0.41
SCMC 20 NP	0.59	0.76	0.84	.91	0.45

Remarkably almost 8.3% SZ was released by SCMC 30 NP within the first 5 minutes which adds up to more than 8 times the reported MIC of SZ against periodontic pathogens<sup>7</sup>. The initial higher burst release of SCMC30NP can be attributed to availability of free nanomeric SZ (E.E of S5 is 77.5±2.3%, rest 22.5 % is available as free SZ). During the process of nanoprecipitation the drug also undergoes nanoprecipitation along with polymer, and so is subject to faster dissolution in accordance with Noyes Whitney's equation. Once free SZ is exhausted, a slower sustained release pattern is observed because SZ now has to traverse a double barrier, first diffuse across polymeric matrix and then across the semi- solid gel structure. Since the degradation period of PCL has been reported to be more than 2 years<sup>26</sup> its erosion promoting SZ release is impossible. 'n' value of less than .5 further substantiates our theory of dominant fickian diffusion controlling SZ transport across the polymeric shell in case of SCMC 30NP.

### 3.9. Anti-Bacterial Well Diffusion Assay

The comparative antibacterial activity of SCMC 30, SCMC 30 NP and SZ solution was evaluated in-vitro by well diffusion method using 20 isolates of *A. actinomycetemcomitans*, the major periodontopathic bacteria. Table 3 shows the measurements on the bacterial plate. The diameter of the growth inhibition zone was directly proportional to the concentration of SZ. However SCMC 30 NP produced significant growth inhibition zones against the oral bacteria tested even in cases where SZ content was as low as 0.1 µg/mL, whereas other groups failed to

produce any response at the same concentration. At higher concentrations of 0.5  $\mu\text{g/mL}$ , SCMC 30 NP caused roughly 1.5 times (64 mm) greater inhibition in comparison to SCMC30 (40mm) and SZ (38mm). McIlvine buffer (pH6.6) used as a negative control showed no inhibitory activity on any of these bacteria. The improved performance of SCMC 30 NP might have its root in the biphasic SZ release profile offered by SCMC 30 NP. The fact that only 70 % of drug is released in first 24 hrs (Figure 4) after application implies that a reservoir of SZ contained by SCMC 30NP is still available to inhibit bacteria during the remaining 48 hours of the well diffusion testing. This reservoir is absent in SCMC 30 and SZ group, probably limiting their antibacterial efficacy.

### 3.10. Clinical Studies

The gel formulations (SCMC 30 and SCMC 30 NP) were effective in reducing periodontal markers. It also controlled localized infection and prevented new lesion formation. The formulations were biologically accepted without any side effects, however taste related issues were reported. The dose frequency was also reduced as once a day dosing was used in our study instead of the usual practise of applying localized antibiotics several times a day.

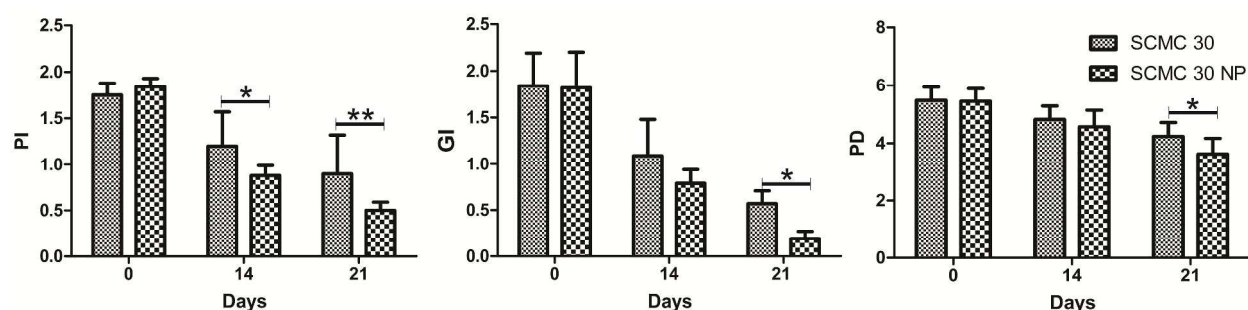


**Figure 5:** Statistical detailing of periodontal markers monitored in the clinical study. Superscript ‘\*’ =  $p < 0.05$ , ‘\*\*’ =  $p < 0.01$  and ‘\*\*\*’ =  $p < 0.001$  vs. SCMC30 obtained after applying two way ANOVA followed by Bon-Ferroni posttests; here  $n=10$  number of patients.

During the study period all the patients showed an improvement in clinical parameters PD, GI and PI. After 21st day, the reading in GI, PD and PI compared to baseline were reduced by about

69%, 23% and 49%, respectively for SCMC 30 and 90%, 33%, and 73% in SCMC 30 NP which shows that SCMC 30 NP gel. At the end of 21st day SCMC 30 NP caused significant ( $P<0.05$ ) decrease in GI, PD as compared to SCMC 30. Also reduction in PI produced by SCMC 30 NP was highly significant ( $P<0.01$ ) as compared to SCMC 30. Recordings of each parameter for SCMC 30 and SCMC 30 NP are statistically depicted in Figure 5.

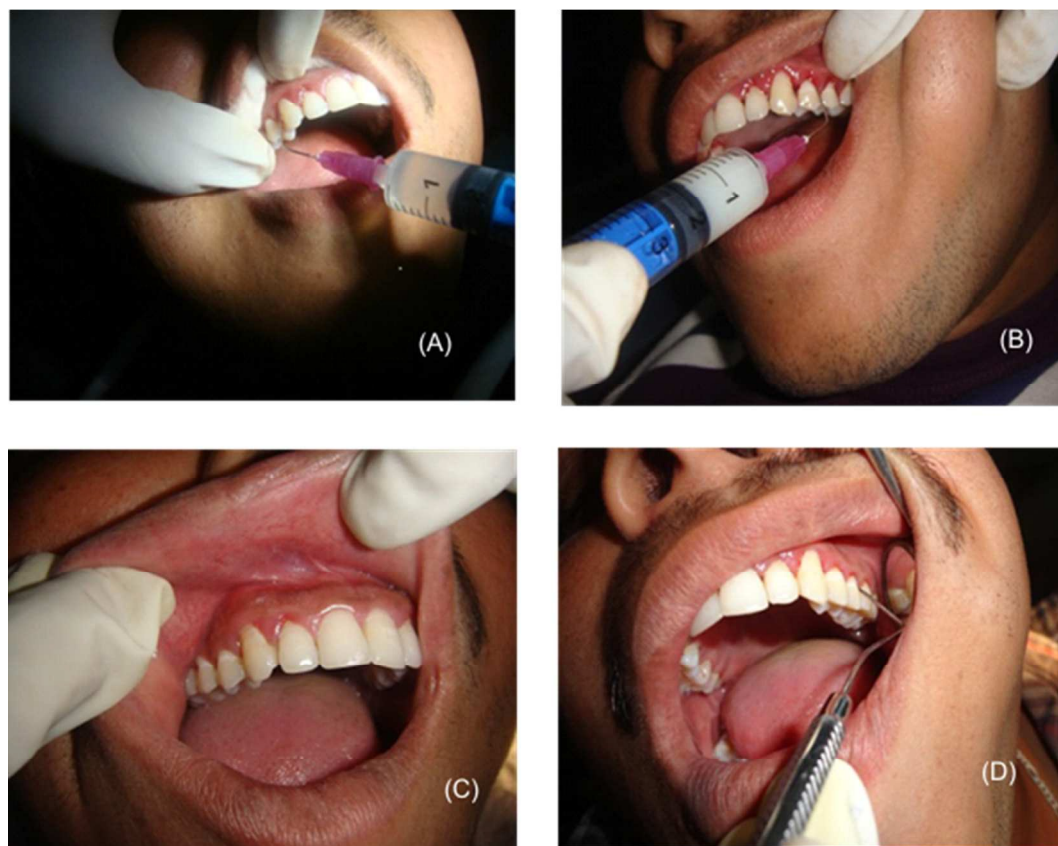


**Figure 6:** Snapshots of a patient undergoing clinical study. The trial was split mouth i.e. locations for groups designated as A and B were both situated in mouth of the same person. (A) SCMC30 and (B) SCMC 30 NP being administered on 0th day; (C) and (D) show level of healing on 21st day in groups A and B respectively. The indentations have filled up, with no evidence of bleeding on probing.

The images presented in Figure 6 are of a single patient. The gravely infected site was deliberately kept in Group B whereas the moderately stressed location was taken in Group A so as to bring about the difference in efficacy of treatment modalities on a visual level. Better recovery is clearly evident at the end of 21st day in group B. Some additional before and after

pictures along with the methodology followed in recording clinical markers during treatment regime have been included in supplementary data sheet.

#### **4. CONCLUSIONS**

The G-PNP were prepared, characterized and incorporated successfully in SCMC based gel. The ability to form a stable aqueous dispersion of SZ was inherently increased by utilizing the G-PNP of SZ, whereas high degree of retention accorded by mucoadhesive nature ensured prolonged drug exposure. The favourable Th-2 biased immunomodulation is expected to offer significant clinical advantage. The formulation system was deemed to be a tremendous success, as it instituted clinical benefits in diseased patients upon applying only once daily. Additionally the formulation was highly user friendly due to its painless, application because of its soft smooth texture. The gel is easy to manufacture on a laboratory scale and should be subjected to scale up on industrial level.

#### **AUTHOR CONTRIBUTIONS**

The manuscript was written through contributions of all authors. All authors have given approval to the final version of the manuscript.

#### **ABBREVIATIONS**

SZ, Satranidazole; MZ, Metronidazole; PNP, Polymeric nanoparticles; G-PNP, ganglioside coated polymeric nanoparticles; PCL, Polycaprolactone; Th1, T helper1; IL-12, Interleukin 12, IL-4, Interleukin 4; TGF- $\beta$ , Transforming growth factor  $\beta$ ; TNF- $\alpha$ , Tumor necrosis factor  $\beta$ ; SCMC, Sodium carboxymethylcellulose; CB934P, Carbopol 934P; HPMC, Hydroxyl propyl methylcellulose; HPC, Hydroxypropylcellulose; HEC, Hydroxyethylcellulose; GD, Disialoganglioside from bovine milk; TEM, Transmission electron microscopy; XRD, X-Ray

diffraction; E.E., Entrapment efficiency; DSC, Differential Scanning Calorimetry; TPA, Texture Profile Analyser.

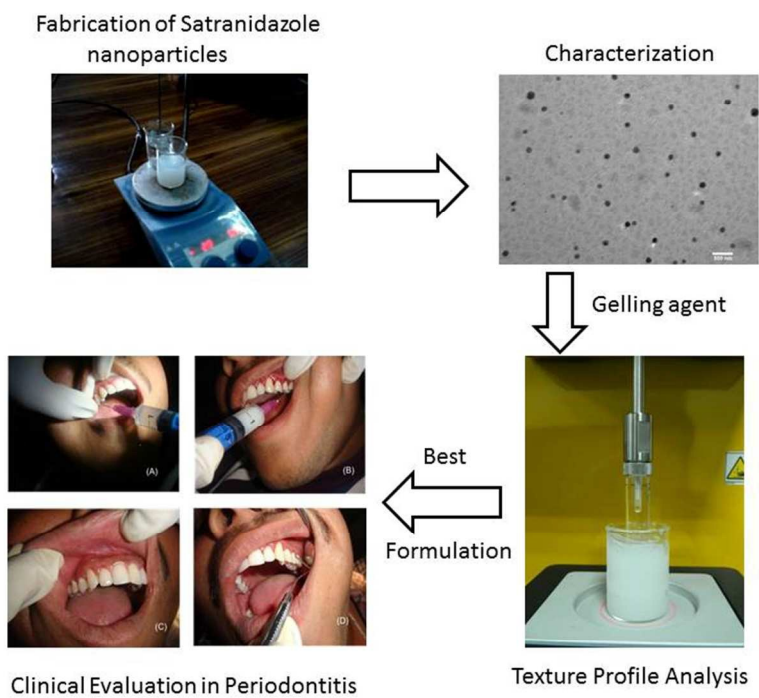
## 5. ACKNOWLEDGMENT

The chemicals and the TEM facility in the experiments were availed using the contingency fund set aside by Indian Institute of Technology, Banaras Hindu University for course work of first author. Authors would also like to thank the financial project UGC-SAP which provided the necessary instrumentation for particle size analysis. The authors would like to express their gratitude towards Dr. Alok Jha, Head, Centre of Food Science & Technology, BHU, for facilitating texture profile analysis.

## REFERENCES

1. G. R. Souto, C. M. Queiroz-Junior, F. O. Costa and R. A. Mesquita, *Immunobiology*, 2014.
2. F. W. M. G. Muniz, C. C. de Oliveira, R. de Sousa Carvalho, M. M. S. M. Moreira, M. E. A. de Moraes and R. S. Martins, *European Journal of Pharmacology*, 2013, **705**, 135-139.
3. R. Laxminarayan, A. Duse, C. Wattal, A. K. M. Zaidi, H. F. L. Wertheim, N. Sumpradit, E. Vlieghe, G. L. Hara, I. M. Gould, H. Goossens, C. Greko, A. D. So, M. Bigdeli, G. Tomson, W. Woodhouse, E. Ombaka, A. Q. Peralta, F. N. Qamar, F. Mir, S. Kariuki, Z. A. Bhutta, A. Coates, R. Bergstrom, G. D. Wright, E. D. Brown and O. Cars, *The Lancet Infectious Diseases*, 2013, **13**, 1057-1098.
4. A. Prakasam, S. S. Elavarasu and R. K. Natarajan, *Journal of pharmacy & bioallied sciences*, 2012, **4**, S252-255.
5. L. Brunton, J. Lazo and K. Parker, *Goodman & Gilman's The Pharmacological Basis of Therapeutics, Eleventh Edition*, 11 edn., Mcgraw-hill, 2005.
6. J. Muzaffar, K. Madan, M. P. Sharma and P. Kar, *Digestive diseases and sciences*, 2006, **51**, 2270-2273.
7. R. Gowrishankar, R. P. Phadke, S. D. Oza and S. Talwalker, *The Journal of antimicrobial chemotherapy*, 1985, **15**, 463-470.
8. K. Bansal, M. K. Rawat, A. Jain, A. Rajput, T. P. Chaturvedi and S. Singh, *AAPS PharmSciTech*, 2009, **10**, 716-723.
9. S. Bisht, G. Feldmann, S. Soni, R. Ravi, C. Karikar, A. Maitra and A. Maitra, *Journal of nanobiotechnology*, 2007, **5**, 3.
10. W. S. Cheow, M. W. Chang and K. Hadinoto, *Pharmaceutical research*, 2010, **27**, 1597-1609.
11. L. H. Alvarenga, R. A. Prates, T. M. Yoshimura, I. T. Kato, L. C. Suzuki, M. S. Ribeiro, L. R. Ferreira, S. A. d. S. Pereira, E. Martinez and E. Saba-Chujfi, *Photodiagnosis and Photodynamic Therapy*.
12. M. Yamamoto, K. Fujihashi, T. Hiroi, J. R. McGhee, T. E. V. Dyke and H. Kiyono, *Journal of Periodontal Research*, 1997, **32**, 115-119.
13. F. A. Crespo, X. Sun, J. G. Cripps and R. Fernandez-Botran, *Journal of Leukocyte Biology*, 2006, **79**, 586-595.

14. H. Fessi, F. Puisieux, J. P. Devissaguet, N. Ammoury and S. Benita, *International Journal of Pharmaceutics*, 1989, **55**, R1-R4.
15. S. I. Bhoir, P. V. Gaikwad, L. S. Parab, R. N. Shringarpure, S. S. Savant and P. J. Verma, *Journal of Chromatographic Science*, 2011, **49**, 84-87.
16. Y.-H. C. Lin, Chiung-Tong; Liang, Hsiang-Fa; Kulkarni, Anandrao R; Lee, Po-Wei; Chen, Chun-Hung; Sung, Hsing-Wen;, *Nanotechnology* 2007, **18**, 1–11.
17. A. Jain, S. K. Singh, Y. Singh and S. Singh, *J Biomed Nanotechnol*, 2013, **9**, 891-900.
18. M. S. Muthu, M. K. Rawat, A. Mishra and S. Singh, *Nanomedicine : nanotechnology, biology, and medicine*, 2009, **5**, 323-333.
19. J. Varshosaz, N. Tavakoli and S. Saidian, *Drug delivery*, 2002, **9**, 127-133.
20. D. S. Jones, A. D. Woolfson and A. F. Brown, *International Journal of Pharmaceutics*, 1997, **151**, 223-233.
21. P. Costa and J. M. Sousa Lobo, *European Journal of Pharmaceutical Sciences*, 2001, **13**, 123-133.
22. M. Fani and J. Kohanteb, *Journal of oral science*, 2012, **54**, 15-21.
23. Y. Singh, P. Ojha, M. Srivastava and M. K. Chourasia, *Journal of Microencapsulation*, **0**, 1-11.
24. Y. Singh, M. Singh, J. G. Meher, V. K. Pawar and M. K. Chourasia, *International Journal of Pharmaceutics*, 2015, **478**, 811-821.
25. C. A. F. Santos, B.D. ; Ghosn, S. ; and Mathiowitz, E., *MRS Proceedings*, 1998, 550-553.
26. J. C. Middleton and A. J. Tipton, *Biomaterials*, 2000, **21**, 2335-2346.



254x190mm (96 x 96 DPI)

### Clinical Relevance

Scientific rationale for study: Periodontitis requires heavy systemic antibiotic dosage with painful mechanical intervention. We have consequently developed a mucoadhesive gel of ganglioside coated nanoparticulate satranidazole.

Principal findings: The intended delivery system slowly released satranidazole in the gingival cavity. Gangliosides modulated the immune response to inhibit inflammatory cytokines and promote anti-inflammatory cytokines. The formulation was verified clinically and ratified by patients and doctors.

Practical implications: It is easy to realize that without the mucoadhesive carrier, delivery system would be quickly washed away. The novelty thus lies in combinatorial utilization of unique properties of nanotechnology, mucodhesive system and immunotherapeutics to come up with once daily dosing regimen.